European Journal of Soil Biology 120 (2024) 103574

Contents lists available at ScienceDirect

European Journal of Soil Biology

journal homepage: www.elsevier.com/locate/ejsobi

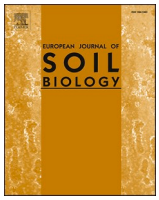

Original article

Quantifying earthworm soil ingestion from changes in vertical bulk density profiles

M. Larsbo [a,*], J. Koestel [a,b], E.J. Krab [a,c], J. Klaminder [c]

[a] Department of Soil and Environment, Swedish University of Agricultural Sciences (SLU), Lennart Hjelms väg 9, 750 07, Uppsala, Sweden
[b] Soil quality and Soil Use, Agroscope, Reckenholzstr. 191, 8046, Zürich, Switzerland
[c] Climate Impacts Research Centre, Department of Ecology and Environmental Science, Umeå University, SE-98107, Abisko, Sweden

ARTICLE INFO

Handling Editor: S. Schrader

ABSTRACT

Soil mixing by earthworms can have a large impact on the fate of nutrients and pollutants and on the soil's ability to sequester carbon. Nevertheless, methods to quantify earthworm ingestion and egestion under field conditions are largely lacking. Soils of the Fennoscandian tundra offer a special possibility for such quantifications, as these soils commonly lack burrowing macrofauna and exhibit a well-defined O horizon with low bulk density on top of a mineral soil with higher density. Since ingestion-egestion mixes the two soil layers, the temporal changes in the bulk density profile of such soils may be useful for estimating field ingestion rates. In this study, we applied a model for earthworm burrowing through soil ingestion to observed changes in soil densities occurring in a mesocosm experiment carried out in the arctic during four summers with intact soil. The earthworms present in the mesocosms were *Aporrectodea trapezoides*, *Aporrectodea tuberculata, Aporrectodea rosea*, *Lumbricus rubellus* and *Lumbricus Terrestris* (fourth season only). We show that changes in soil density profiles can indeed be used to infer earthworm ingestion rates that are realistic in comparison to literature values. Although uncertainties in parameter values were sometimes large, the results from this study suggest that soil turnover rates and endogeic earthworm soil ingestion rates in tundra heath and meadow soils may be as high as those reported for temperate conditions. Such large ingestion rates can explain observed large morphological changes in arctic soils where dispersing earthworms have resulted in complete inmixing of the organic layer into the mineral soil. Our approach is applicable to soil profiles with marked vertical differences in bulk density such as the soils of the Fennoscandian tundra where earthworms are currently dispersing into new areas and to layered repacked soil samples that are incubated in the field.

1. Introduction

Earthworm activities that restructure soils have fascinated researchers since the pioneering work conducted by Charles Darwin in the late 19th century [1]. It is now well-known that earthworm burrowing not only influences water flow, water storage, solute transport and aeration in soils [2,3], but also induces soil mixing with relevance for soil nutrient pools [4], the fate of soil pollutants [5], the physical protection of soil carbon [6,7] and recovery from soil compaction [8].

Although many of the effects of earthworm burrowing on soil processes are well understood, quantitative data needed to link earthworm abundance to ecosystem functions are generally lacking [9]. This is because earthworm burrowing is inherently difficult to observe and quantify due to the opaque nature of soil. Nevertheless, earthworm burrowing has been quantified in laboratory settings using 2D terraria (e.g. Refs. [10–12]) and in short-term 3D mesocosm studies [13–16]. While 2D-approaches allow direct observations of actual worm movements, the 'unnatural' settings in these experiments, where horizontal movements of the earthworms are restricted, make results from such experiments difficult to extrapolate to natural soils. X-ray tomography has been used to quantify the 3D networks of earthworm burrows, but most studies of this kind have been carried out on repacked soil using small soil volumes (about 6 dm^3) that fit in standard medical and industrial X-ray scanners. Therefore, it is not clear how representative estimates of burrowing rates from these experiments are for field conditions.

Earthworm burrowing rates can also be inferred from the vertical redistribution of particles or solutes [17–19] and it has been suggested

* Corresponding author.
E-mail address: mats.larsbo@slu.se (M. Larsbo).

https://doi.org/10.1016/j.ejsobi.2023.103574
Received 16 March 2023; Received in revised form 14 November 2023; Accepted 21 November 2023

that earthworms are especially important for the transport of otherwise immobile or strongly adsorbing substances in soil [20–22]. Hence, earthworm mediated transport has been included in models for arsenic, caesium and lead transport in soil [22–24]. Many of these models use an extended version of the convection-dispersion equation, which includes biodiffusion, to model soil mixing by endogeic earthworms. Biodiffusion rates can be estimated by fitting these models to observed vertical distributions of the elements with depth. Earthworm ingestion rates can then be calculated from the biodiffusion rates [25]. Meurer et al. [26] developed a model that simulates soil structure dynamics with the focus on how biological activity (e.g. microbial activity, root growth and faunal activity) change soil porosity and pore size distributions. They applied their model to an extensive data set including soil water retention measured during a four-year period of soil recovery from compaction [27]. Since the data used for model evaluation was from plots that were free from plants they assumed that earthworms were the main drivers of the observed changes in pore size distributions. However, earthworm activity and plant root growth are interacting processes under natural conditions. It is, therefore, crucial to conduct experiments with both natural plants and earthworms together when estimating realistic soil mixing rates [28].

One simple soil property that has been shown to be affected by earthworms is bulk density [29,30], but to date no study has explored the use of density changes as a proxy for soil mixing induced by earthworms. Therefore, the objective of this study was to evaluate the possibilities of using temporal changes in soil bulk density profiles to estimate earthworm ingestion rates under field conditions. To achieve this, we developed a simple model of the vertical redistribution of soil occurring as an effect of earthworm soil ingestion and egestion and applied it to data from a four-year long mesocosm experiment (including soil and living plants) to which earthworms of different ecological groups were added. The density profiles, which had a well-defined boundary between an organic rich surface layer and the underlying mineral soil in the control experiments (soils without earthworms), were estimated from X-ray tomography images of soil cores at the end of the experiment.

2. Materials and methods

2.1. Experimental data

We used data from a mesocosm (50 × 39 × 30 cm) experiment with partially intact soil from Kärkevagge in northern Sweden described in Blume-Werry et al. [31]. The experiments were carried out in the experimental garden of the Abisko Scientific Research Station and included two different vegetation types (heath n = 24; and meadow n = 24). These two vegetation types, which are common in the Arctic, are dominated by dwarf shrubs and graminoids (heath) and forbs (meadow) [31,32]. For both vegetation types an approximately 22-cm thick layer of homogenised mineral soil was overlain by an 8-cm thick layer of intact organic soil including natural vegetation. The organic matter contents (OC) in this O-horizon for the heath and the meadow were 69 and 60 % for the control at the end of the experiments. The corresponding data for the earthworm treatment were 74 and 38 % [28]. Soil pH measured in water was on average 4.5 and 5.2 for the heath and meadow, respectively [28]. The soil was left to settle during the 4-year period from mesocosm installation in 2013 to the introduction of earthworms in summer 2017.

A total fresh weight of 24.2 g ± 0.3 (mean ± SE) of earthworms were added to each mesocosm each year. Since the depth of the mesocosms was limited to 30 cm all earthworms died during winters. The earthworms were adult Aporrectodea species (*Aporrectodea trapezoides*, *Aporrectodea tuberculata, Aporrectodea rosea*, 16–17 individuals per mesocosm) and adult *Lumbricus rubellus* (27–29 individuals per mesocosm), corresponding to densities of 87 and 140 individuals m^{-2}, respectively. In 2020 one adult *Lumbricus terrestris* (about 4 % of the mass of added earthworms) was added to each mesocosm. As a comparison earthworm densities, dominated by Aporrectodea species are currently dispersing from anthropogenic sources in the area around Abisko with earthworm densities often exceeding 200 individuals m^{-2} [33]. The Aporrectodea species included in this study belong to the endogeic ecological category while *Lumbricus rubellus* is commonly classified as epigeic and *Lumbricus terrestris* is classified as anecic. However, it is uncommon that earthworm species belong 100 % to any of the three main ecological categories [Bouché 34, 35]. For example, *Lumbricus rubellus* is according to a revised classification scheme proposed by Botinelli et al. [35] 85 % epigeic and 15 % anecic. This intermediate ecological behaviour of *Lumbricus rubellus* was also stressed by Briones and Álvarez-Otero [36]. The average weight of an earthworm in the mesocosm experiment during the first three summers was 24.4/44 = 0.555 g. Assuming a length to diameter ratio of 20 and a density of 1 g cm^{-3}, the average worm diameter was 3.3 mm.

At the end of the experiment in September 2020, 48 intact cores with diameters of approximately 10 cm and heights between 10 and 20 cm were sampled from all mesocosms. 3D X-ray tomography images of all samples were recorded and processed as described in Klaminder et al. [28]. Examples images for the vegetation types and treatments show casts of high density (bright) in the organic rich layer for the earthworm treatments (Fig. 1b and d) that are not apparent in the controls (Fig. 1a and c). One average soil bulk density profile for each soil and treatment was obtained from the calibrated X-ray images. The depths of the boundary between the two soil layers defined by the maximum gradient in density, were aligned before averaging [28]. Since depth distributions of water contents were not available we assumed a linear relation between image grey values and dry soil bulk density. The relative densities obtained from the X-ray images were scaled using data from standard measurements of dry bulk densities for the organic layer (0.2 g cm^{-3}) and the mineral layer (1.4 g cm^{-3}) of the two soils.

2.2. Modelling approach

The vertical transport of elements due to bioturbation by soil fauna has often been modelled as a diffusive process [22,23,37]. Optimal biodiffusion rates from calibrations can then be related to biological parameters such as soil consumption rates [25]. A more explicit approach was used in Meurer et al. [26] who directly used soil ingestion rate as a model parameter when they modelled the changes in pore size distributions induced by earthworm ingestion and egestion. Here, we use a similar approach although our focus is on changes in soil bulk density rather than changes in pore size distributions. One important difference between the approaches is that, in our case, we model a soil profile where bulk densities change both with depth and time.

Our modelling domain is a 1D soil profile. We modelled two types of earthworm burrowing behaviour (anecic and endogeic) although it is clear that the burrowing behaviour within these ecological categories may differ between species [38]. For convenience, in the following we write “anecic earthworms” and “endogeic earthworms” although what we model is the effects of typical anecic and endogeic behaviour. Even though some of the species added to the mesocosms may have shown epigeic behaviour this was not considered in the model because it would not have influenced bulk densities on the soil profile scale. Both anecic and endogeic earthworms were assumed to ingest and egest soil in a layer from the soil surface down to a depth, L (m), set to 30 cm (i.e. the thickness of the mesocosms). The soil mass ingestion rates for anecic, I_A (kg soil m^{-2} d^{-1}), and for endogeic earthworms, I_E (kg soil m^{-2} d^{-1}), were constant within this depth. Since the soil density was varying with depth the volume of ingested soil also varied. It is known that soil bulk density influences ingested soil volumes [12,16]. However, effects of soil bulk density on the ingested mass of soil appear to be smaller [12]. For simplicity, we assumed that the density did not influence the soil mass ingestion rates. Anecic earthworm ingestion was assumed to create permanent vertical burrows and they were assumed to egest only at the

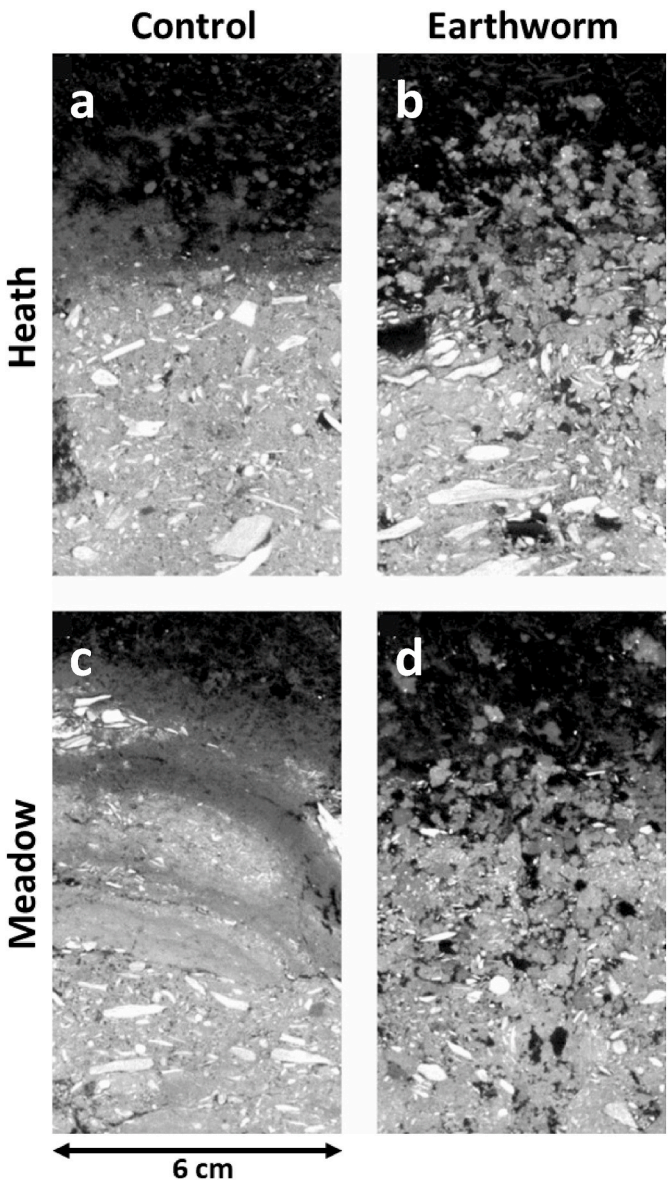

Fig. 1. Examples of vertical slices (X-ray images) through the columns for the control (left) and the earthworm treatment (right) for the heath (top) and meadow (bottom).

soil surface, thereby creating a cast layer. The result of anecic ingestion is, thus, a decrease in mass and density at the point of ingestion while the thickness of the soil layers remains constant except for the cast layer at the soil surface. Burrows from endogeic earthworms are less stable [39]. In our model they were assumed to immediately collapse or fill with cast after creation. This may seem like a strong assumption but it is not critical for the modelling results at the end of the simulation period. Most earthworm burrows created by endogeic soil ingestion will in the long-term perspective collapse or refill with casts. If this was not the case, assuming that endogeic worms egest in the soil, the bulk soil volume would increase and an accompanying elevation of the soil surface would occur. Modelled endogeic ingestion, hence, removes soil from a numerical layer, thereby decreasing the mass and thickness while leaving the density unaffected. In a 1D model only the vertical component of earthworm burrowing is accounted for. The vertical component of 3D isotropic burrowing (i.e. earthworms were assumed to burrow in all directions with equal probability) is 0.5 [25]. The total endogeic ingestion rate was, hence, given by multiplying the modelled 1D ingestion rate with 2 [25]. Endogeic earthworms were assumed to egest soil in the vicinity of the point of ingestion. Soil of a given density is, hence, distributed around the point of ingestion resulting in an increase in mass and thickness. The density in these layers will either remain unchanged, increase or decrease depending on the density of the egested soil (see below) and the density of the resident soil in the layer. The spread in egestion by endogeic earthworms is defined by the egestion radius parameter (i.e. the number of layers in each vertical direction from the layer of ingestion), e_{radius} (n layers). The likelihood of egestion was assumed to be uniform within the volume defined by the egestion radius. The combined effect of endogeic ingestion and egestion in a layer is a change in density and thickness while mass is conserved. Earthworms can also move through soil by cavity expansion (i.e. pushing the soil aside). This process was not included in the model, mainly because it does not lead to soil mixing on the soil profile scale. However, we acknowledge that cavity expansion changes bulk density locally, where soil along burrows is compacted [40]. If burrows created by cavity expansion collapse it will lead to an increase in average bulk density. This was not seen in our measured data, which show an average decrease in bulk densities (Fig. 2).

For each numerical soil layer i the mass, m (kg m^{-2}), layer thickness, T (m) and dry bulk density, ρ (kg m^{-3}), at time $j+1$ are given by:

$$m_i^{j+1} = m_i^j + m_{egE,i} - m_{ingA,i} - m_{ingE,i} \quad \text{Eq. 1}$$

$$T_i^{j+1} = T_i^j + T_{egE,i} - T_{ingE,i} \quad \text{Eq. 2}$$

$$\rho_i^{j+1} = \frac{m_i^{j+1}}{T_i^{j+1}} \quad \text{Eq. 3}$$

where the subscripts *ingA*, *ingE and egE* denotes anecic ingestion, endogeic ingestion and endogeic egestion, respectively. The ingested masses are given by:

$$m_{ingA,i} = \Delta t\, f_i I_A \quad \text{Eq. 4}$$

$$m_{ingE,i} = \Delta t\, f_i I_E \quad \text{Eq. 5}$$

where Δt is the timestep and f_i (−) is the fraction of the total mass contained in layer i.

$$T_{ingE,i} = \Delta t \frac{m_{ingE,i}}{\rho_{ingE,i}} \quad \text{Eq. 6}$$

$$m_{egE,i} = \sum_{layer=i-e_{radius}}^{layer=i+e_{radius}} \frac{m_{ingE,k}}{2e_{radius}+1} \quad \text{Eq. 7}$$

$$T_{egE,i} = \Delta t \frac{m_{egE,i}}{\rho_{cast}} \quad \text{Eq. 8}$$

where ρ_{cast} (kg m^{-3}) is the dry bulk density of the casts.

Soil ingested close to soil surface or bottom of the profile is not allowed to be egested outside of the model domain boundaries. To preserve mass in each layer, the soil that should, according to the e_{radius} value, have been egested outside the modelling domain was instead egested at the point of ingestion.

Both the chemical and physical properties of the casts differ from the ingested soil [41,42]. These changes in properties have been shown to be species dependent [43]. Bottinelli et al. [44] studied the properties of casts from the anecic earthworm *Amynthas khami* in 19 locations in northern Vietnam in relation to the properties of the ingested soil. They found the casts had lower density than the ingested soil if the density of the soil was large and vice versa. Similar results were presented by Barré et al. [45] who showed that earthworm ingestion and egestion decreased the density of compacted soil while the opposite was true for loose soil. We do not have any information on the physical properties of the casts created in our mesocosms. In line with the results cited above, we assume that the density of the casts is a function of the density of the

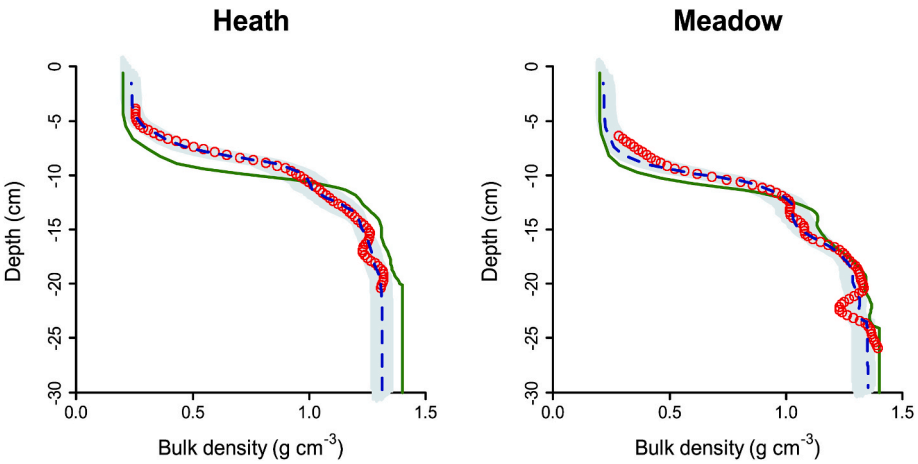

Fig. 2. Dry bulk density (ρ) profiles for initial conditions (dark green line), measured final for earthworm microcosms (open red circles), results from the optimal simulation (dashed blue line) and the interval of accepted simulations (light grey band) for the heath (left) and meadow (right).

ingested soil according to:

$$\rho_{cast} = \rho_{ing} + k\left(\rho_{average} - \rho_{ing}\right) \quad \text{Eq. 9}$$

where $\rho_{average}$ (kg m^{-3}) is the average dry bulk density of the soil and k (−) is a coefficient that determines the magnitude of the change from the ingested soil to the cast.

The analysed regions of interest of the grey-scale images that were used to create the bulk density profiles varied in size between replicates, vegetation type and treatment [28]. It was, therefore, not possible to determine the actual depth from the soil surface to the transition zone between the organic rich topsoil and the underlying mineral soil. To enable comparison between measured and modelled density profiles we introduced a parameter, V_{offset} (m) that corrected for any vertical offset between simulated and measured data.

The model code written in R [46] will be made available upon request.

2.3. Model evaluation

Both the number of earthworms, due to mortality and reproduction, and their activity, due to differences in soil moisture and temperature, likely varied during the summers. Since we did not have data on these eventual changes we assumed that ingestion and egestion rates were constant with time during the four-months periods following the introduction of the worms. Hence, modelled soil consumption rates are averages for the total simulated period of 16 months.

Model outputs were bulk densities in discrete numerical layers with varying thickness. Since the thicknesses vary with time, the simulated depths to a layer at the end of a simulation is dependent on model parameter values. We used natural cubic splines (splinefun in R; 46) to interpolate the measured data. Measured data at depths corresponding to the simulated depths were then estimated from the resulting spline function and used for quantitative model evaluation.

The measured data on bulk densities for the control treatment were used as initial conditions. However, soil mesofauna contribute to soil mixing [47]. This means that also the density profiles of the control treatments may have changed during the experiment. We do not know the bioturbation rate of the mesofauna in the mesocosms during the experimental period. However, we were interested in modelling the effects of earthworms, which is the difference between the control and the earthworm treatment assuming that any effects of the mesofauna was similar for the two treatments.

The model was calibrated against measured data from the earthworm treatment. All five parameters (I_A, I_E, e_{radius}, k and V_{offset}) were included in the calibration. We used latin hypercube sampling ("lhs" package in R; 46) to generate 100000 parameter value combinations within predefined initial parameter intervals. The initial parameter intervals were determined from preliminary Monte Carlo runs with the model. Root mean square errors (RMSE) between final simulated values and interpolated measured values of bulk density were calculated. The parameter set that resulted in the smallest RMSE is in the following referred to as the optimal parameter set. We accepted all simulations that resulted in an RMSE smaller than the thresholds of 0.035 and 0.045 for the heath and the meadow, respectively. These thresholds were chosen because they resulted in posterior parameter uncertainty 'envelopes' of accepted simulations that covered most of the measured data. An estimate of the uncertainty in the parameter values after calibration, U (−), was obtained by dividing the posterior parameter value range with the midpoint of the parameter range according to:

$$U = \frac{L_{upper} - L_{lower}}{\left(L_{upper} + L_{lower}\right)/2} \quad \text{Eq. 10}$$

where L_{upper} and L_{lower} are the upper and lower boundaries of the posterior parameter interval, respectively.

In experiments designed for model evaluations, the depth of the profile or the elevation of the soil surface should be monitored and a parameter describing the vertical offset between measured and modelled data would not be needed. To evaluate parameter identifiability for such a case, a second calibration was run with the vertical offset set to the optimal values (i.e. the value resulting in the smallest RMSE) from the first calibration. Thus, only four parameters were included in this calibration. Finally, all parameters except the endogeic ingestion rate were set to optimal values and another calibration was carried out.

2.4. Sensitivity analysis

A simple measure of sensitivity was calculated as the root mean square difference (RMSD) between the optimal simulation and simulations where the parameter values for the optimal parameter set (5-parameter calibration) were increased by 10 % one-at-a-time.

2.5. Estimations of burrowing rates

We estimated endogeic burrowing rates (cm d^{-1}) in the organic and mineral layers from the known masses of the worms, the optimum parameter values for endogeic ingestion rates and the densities of the soil layers. To do this we assumed that the volume of soil ingested could be approximated by a cylinder with the same diameter as the average diameter of the worms (3.3 mm).

3. Results

3.1. Model performance and earthworm ingestion

Fig. 2 shows that the optimal simulations for the model with five parameters reproduced the measured bulk density depth profiles satisfactorily both for the heath (RMSE for optimal simulations was 0.027) and the meadow (RMSE for optimal simulations was 0.11). The model could not reproduce the fluctuations in measured values between 15 and 20-cm depth for the heath and between 20 and 25-cm depth for the meadow. These fluctuations may be effects of the limited depth of the mesocosms, effects that were not accounted for in the model. Optimal parameter values for the calibration with all five parameters are presented in Table 1. The optimal parameter values for the endogeic ingestion rates (I_E) were 240 and 140 g dry soil m^{-2} d^{-1} for the heath and the meadow, respectively. The masses of dry soil in the 30 cm layer calculated from the density profiles were 296 and 270 kg m^{-2}. When accounting for the horizontal component of the earthworm burrowing these values correspond to a yearly soil turnover by earthworms of 19 and 12 % for the heath and the meadow. The corresponding consumption rates were 3.8 and 2.2 g dry soil g^{-1} fresh worm. The burrowing rates for the endogeic worms in the mineral soil were 18 and 10 cm d^{-1}. The optimal values for the endogeic egestion radii (e_{radius}) were 23 and 27 numerical layers for the heath and meadow, respectively. This corresponds to vertical distances of 4.1 and 4.3 cm in the mineral soil. Optimal values for the anecic ingestion rates (I_A) were 18 and 3.0 g dry soil m^{-2} d^{-1} for the heath and the meadow, respectively. This corresponds to 2.9 and 0.53 % of the soil being ingested by anecic earthworms during the simulation time (16 months). The corresponding thicknesses of the cast layers resulting from anecic egestion were 8.8 and 1.5 mm. The coefficients governing the density change from soil to cast (k) were 0.21 and 0.30 for the heath and the meadow. Optimal parameter values for the calibration with reduced number of parameters were similar to those for the calibration with all five parameters (Tables 1–3).

Table 1
Summary of calibration results for the heath and the meadow. All five model parameters were included.

Parameter	Initial uncertainty interval	Interval accepted parameter combination	Optimal parameter value	Uncertainty estimate, U
Heath				
Endogeic ingestion rate, I_E (g cm^{-2} d^{-1})	0–0.05	0.007–0.046	0.024	1.5
Anecic ingestion rate, I_A (g cm^{-2} d^{-1})	0–0.01	0–0.0048	0.0018	2.0
Vertical offset, V_{offset} (cm)	-1–3	0–2.2	1.3	1.0
Egestion radius, e_{radius} (n_layers)	3–45	12–31	23	0.88
Density change coeff., k (−)	0–0.5	0–0.43	0.21	2.0
Meadow				
Endogeic ingestion rate, I_E (g cm^{-2} d^{-1})	0–0.05	0.002–0.05	0.014	1.9
Anecic ingestion rate, I_A (g cm^{-2} d^{-1})	0–0.01	0–0.0040	0.0003	2.0
Vertical offset, V_{offset} (cm)	-1–3	−0.5–2.0	1.0	3.2
Egestion radius, e_{radius} (n_layers)	3–45	3–43	27	1.7
Density change coeff., k (−)	0–0.5	0–0.5	0.30	2.0

3.2. Parameter sensitivity and uncertainty

With the chosen thresholds, the posterior uncertainty intervals (the grey bands in Fig. 2) covered 100 and 87 % of the measured data for the heath and the meadow, respectively. Fig. 3 shows the RMSE values for the Monte Carlo simulations plotted against the values of each of the five parameters. Parameter values for the accepted simulations were generally more constrained for the heath than the meadow. This can also be seen in the smaller values of the uncertainty estimates for the heath (Table 1). The range of parameter values for the endogeic ingestion rate (7–46 g dry soil m^{-2} d^{-1}) for the heath corresponds to a range in consumption rates of 1.1–7.3 g dry soil g^{-1} fresh worm d^{-1}. The initial uncertainty range was only marginally decreased for the endogeic ingestion rate for the meadow and hence the calibration provided no guidance on consumption rates.

Posterior uncertainty intervals were generally smaller when the

Table 2
Summary of calibration results for the heath and the meadow. The vertical offsets were set to the optimal values.

Parameter	Initial uncertainty interval	Interval accepted parameter combination	Optimal parameter value	Uncertainty estimate, U
Heath				
Endogeic ingestion rate, I_E (g cm^{-2} d^{-1})	0–0.05	0.015–0.040	0.023	0.89
Anecic ingestion rate, I_A (g cm^{-2} d^{-1})	0–0.01	0–0.0032	0.0017	2.0
Egestion radius, e_{radius} (n_layers)	3–45	13–31	21	0.82
Density change coeff., k (−)	0–0.5	0.11–0.40	0.21	1.2
Meadow				
Endogeic ingestion rate, I_E (g cm^{-2} d^{-1})	0–0.05	0.009–0.049	0.015	1.4
Anecic ingestion rate, I_A (g cm^{-2} d^{-1})	0–0.01	0–0.0027	0.0003	2.0
Egestion radius, e_{radius} (n_layers)	3–45	3–43	31	1.7
Density change coeff., k (−)	0–0.5	0.08–0.50	0.26	1.5

Table 3
Summary of calibration results for the heath and the meadow when all parameters except the endogeic ingestion rates were set to optimal values.

Parameter	Initial uncertainty interval	Interval accepted parameter combination	Optimal parameter value	Uncertainty estimate, U
Heath				
Endogeic ingestion rate, I_E (g cm^{-2} d^{-1})	0–0.05	0.016–0.030	0.023	0.60
Meadow				
Endogeic ingestion rate, I_E (g cm^{-2} d^{-1})	0–0.05	0.010–0.019	0.014	0.62

vertical offset was set to the optimal value (Table 2). For example, the endogeic consumption rates corresponding to the posterior parameter uncertainty range for the endogeic ingestion rate for the heath were reduced to 2.4–6.3 g dry soil g^{-1} fresh mass d^{-1}.

Setting all parameter values except the endogeic ingestion rate to optimal values further reduced the posterior parameter uncertainty compared to the calibrations with four and five parameters (Table 3). For this case, endogeic consumption rates for the heath were in the range 2.5–4.8 g dry soil g^{-1} fresh worm d^{-1}.

The accepted parameter values were significantly correlated for many of the parameters (Fig. 4). The sensitivity analysis showed that the bulk density profiles were most sensitive to changes in the endogeic ingestion rate and the vertical offset and least sensitive to changes in the anecic ingestion rate, especially for the meadow (Table 4). The differences in sensitivity between the heath and the meadow were minor for all parameters except the anecic ingestion rate.

4. Discussion

Previous studies suggest that under favourable environmental conditions, up to c. 20–25 % of the total topsoil mass can be ingested each year by earthworms, predominantly by endogeic species [48,49]. Soil consumption rates of 1.0–2.5 g dry soil g^{-1} fresh mass d^{-1} appear to be typical for temperate geophagous species [40]. Meurer et al. [26] found through calibration that the consumption rate was 2.79 g dry soil g^{-1} fresh mass d^{-1} for their study on compaction recovery. Ingestion rates and consumption rates calculated from the optimal parameter values in our study using two different tundra soils were in the range of these previously reported values for temperate soils or slightly higher. The possibility of higher ingestion rates are somewhat surprising considering that earthworms are believed to generally consume less soil in cold conditions [50]. However, our optimal parameter values seem realistic from a perspective of soil morphological changes observed at a nearby earthworm invasion gradient. For example, our inferred ingestion rates, which suggest a decadal timescale for the turnover of the topsoil (i.e. 19 and 12 % of the soil was ingested annually for the heath and the meadow), could explain morphological observations in arctic soils where dispersing earthworms have been found to cause complete inmixing of the O horizon into the mineral soil since the introduction of earthworms [33].

Reported average burrowing rates for endogeic earthworms are in the range 6–15 cm d^{-1} [12,14,51]. Endogeic burrowing rates in the mineral soil calculated from optimal simulated values were within this interval or slightly higher. It should be noted that the uncertainty in estimated burrowing rates is larger than for turnover rates and ingestion rates because it includes also uncertainties in burrow diameter.

The fractions of the soil that were ingested by anecic earthworms calculated from optimal ingestion rates were small compared to the earthworm generated macroporosities in the mineral soil of 5.2 % [28]. One possible explanation is that some of the burrows created by endogeic earthworms, especially those created during the fourth summer, remained intact (i.e. did not fill with casts or collapse during the experiment).

We are not aware of any data on distances between the point of soil ingestion and egestion. However, the vertical distances (e_{radius}) of 4.1 and 4.3 cm for the heath and the meadow calculated from the optimal values for endogeic egestion radii are comparable to the assumed average earthworm length of 6.5 cm. Earthworms may move either by ingesting soil or by pushing the soil to the sides (cavity expansion). Information on the ratio between these modes of burrowing would be needed to verify that these estimates are reasonable. Similarly, we do not have measured data on soil density changes from ingestion to egestion available for comparison. In future studies, the bulk density of casts should be measured to help constrain the values of remaining calibrated parameters.

Our results suggest that ingestion rates were higher in the heath than in the meadow mesocosms. The reasons for this are not clear but these results are in line with the larger effects of earthworms on macropore network characteristics and on plant N uptake compared to the meadow [28,31]. One plausible explanation for the lower ingestion rates in the mineral soil of the meadow is that a considerable part of the earthworm's activity in this vegetation type occurred in the litter layer. This explanation is supported by observation of more substantial losses of litter from the meadow mesocosms compared to the heath [31]. The model could generally reproduce the measured data better for the heath than for the meadow. A larger threshold for accepted simulations for the meadow was used to widen the envelope of accepted simulations and thereby cover most measured data points. This can at least partly explain the better-constrained parameter values for the heath compared to the meadow.

The posterior uncertainty intervals were large, especially for the calibration including all five parameters. There are two main reasons why parameter values could not be further constrained by calibration: i) the model output, in this case the density profiles, were insensitive to changes in parameter values, and/or ii) parameter values for accepted simulations were correlated. For example, neither the endogeic ingestion rate (I_E) nor the endogeic egestion radius (e_{radius}) were insensitive parameters. Nevertheless, it was not possible to constrain the values of these parameters since these parameters have similar effects on final simulated density profiles (i.e. large values result in more smoothing). The anecic ingestion rate (I_A) and the density change parameter (k) also have partly similar effects on the density profiles. Large values for I_A moves the simulated density profile towards smaller densities while large values of k decreases the range between the small densities at the top of the profile and the large densities at the bottom. This results in a negative correlation between these parameters (Fig. 4). Additionally the low sensitivity of I_A further limits the identifiability for this parameter. Posterior uncertainty intervals for the calibrations with known vertical offset were still large due to correlations between the accepted parameter values (Fig. 4). Significant reductions in the uncertainty for the endogeic ingestion rate when all other parameters were set to optimal values show that independent measurements that reduce the initial parameter intervals could improve parameter identifiability.

The model used in this study is simple (two categories of earthworm behaviour including permanent/collapsing burrows, uniform ingestion in the modelling domain and uniform egestion within the egestion radius). Indeed, many more processes could have been included in the model. However, it is important to highlight that more advanced modelling approaches would generally include more parameters that are difficult or impossible to measure directly, and thereby increase problems with non-uniqueness. As far as we know this is the first study that includes estimations of uncertainty in parameter value estimates (uniqueness) for earthworm soil ingestion-egestion modelling.

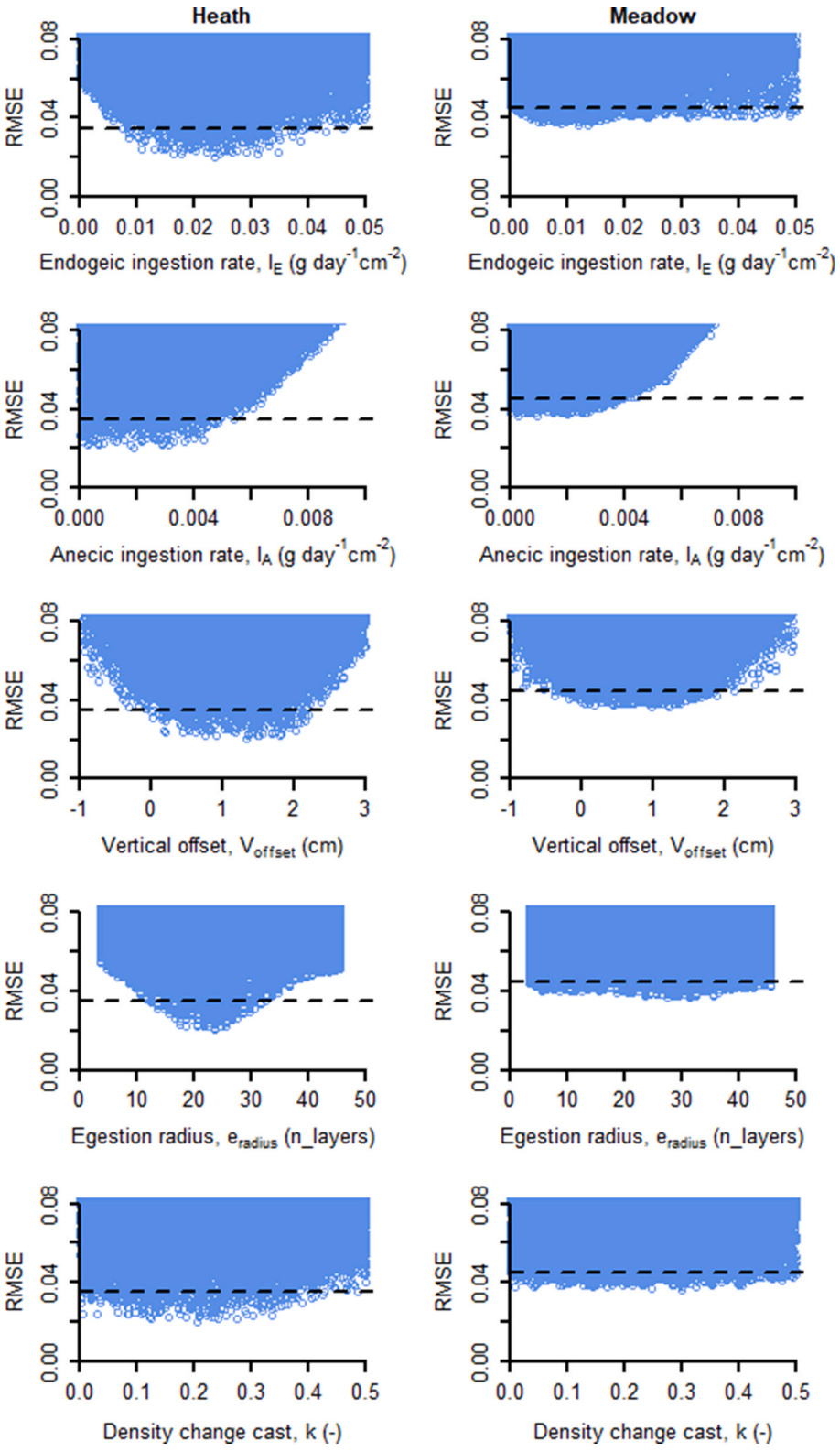

Fig. 3. Root mean square errors (RMSE) between measured and simulated bulk densities for the heath (left column) and meadow (right column) soils.

Considering the complexity and number of parameters in previously published models it seems likely that posterior parameter uncertainty would be large also for these models.

The modelling approach presented here should not be viewed as a universal method for estimating earthworm soil ingetstion. However, the use of temporal changes in bulk density profiles is a promising addition to the already existing toolbox where each method to infer ingestion rates has its advantages and disadvantages. One obvious disadvantage with the approach taken in this study is that many soils are rather homogeneous with depth and temporal changes in density depth distributions due to bioturbation will be negligible. The main advantage with our approach is that earthworm ingestion and egestion often

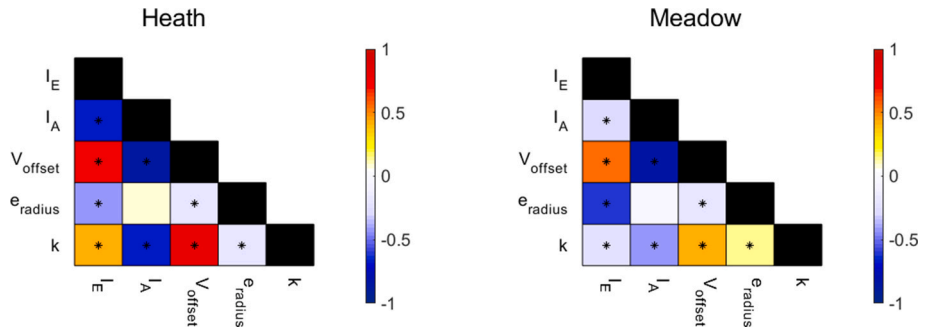

Fig. 4. Pearson correlation coefficients for parameter values of the accepted simulations for the heath (left) and meadow (right) soils for the calibration including all five parameters Asterisks denote significant correlation at p = 0.05. I_E, endogeic ingestion rate; I_A, anecic ingestion rate; V_{offset}, vertical offset; e_{radius}, endogeic egestion radius; k, density change coefficient cast.

Table 4
Results from sensitivity analysis. RMSD is the root mean square deviation between the optimal simulation and simulations where the parameter values were increased by 10 % one-at-a-time.

Parameter	RMSD	
	Heath	Meadow
Endogeic ingestion rate, I_E (g cm^{-2} d^{-1})	0.0097	0.0088
Anecic ingestion rate, I_A (g cm^{-2} d^{-1})	0.0030	0.00053
Vertical offset, V_{offset} (cm)	0.0094	0.0091
Egestion radius, e_{radius} (n_layers)	0.0064	0.0047
Density change coeff., k (−)	0.0049	0.0042

dominate soil displacement at the soil profile scale [8] and, hence, will be the main driver for changes in density profiles in most types of terrestrial ecosystems in northern Europe. For the other types of data to which earthworm modelling approaches have been applied, other processes than bioturbation may be equally important [22,23,26]. For example, it may be difficult to separate the effects of bio-diffusion from effects of advective-diffusive solute transport in soil water on the displacement of contaminants. Likewise, it may be difficult to separate the effects of bioturbation on temporal changes in pore size distributions from effects of other biological processes (e.g. root growth and decay) and physical processes (e.g. swelling and shrinking, freezing and thawing).

In this study we used bulk density profiles estimated from X-ray tomography images. This kind of data has a very fine spatial resolution and, additionally, contains information on macroporosity and other macropore network properties [28]. Although X-ray data are preferable for calibration of the model presented in this study, it is in principle possible to use simpler standard methods for dry bulk density estimations (i.e. drying and weighing of intact samples with known volume) to generate bulk density depth distributions.

5. Conclusions

We have shown that changes in soil density profiles can be used to infer earthworm ingestion rates for heath and meadow tundra soils. The results from this study suggest that soil ingestion rates for endogeic earthworms in tundra soils may be as high as those reported for temperate conditions. However, we have also shown that the uncertainties in estimated soil turnover rates, consumption rates and burrowing rates are large. These uncertainties could be reduced if more information on, for example, the distances between the point of ingestion and egestion and the density of casts would be available. The modelling approach shows promise for quantifying earthworm consumption rates in soil profiles with marked differences in bulk densities with depth such as the soils of the Fennoscandian Tundra where earthworms are currently dispersing into new areas.

Funding

This study was financed by FORMAS grant no: 2018–01312.

Declaration of competing interest

The authors declare that they have no known competing financial interests or personal relationships that could have appeared to influence the work reported in this paper.

Data availability

Data will be made available on request.

References

[1] C. Darwin, The Formation of Vegetable Mould, through the Action of Worms, with Observations on Their Habits, John Murray, London, 1881.
[2] P. Lavelle, D. Bignell, M. Lepage, V. Wolters, P. Roger, P. Ineson, O.W. Heal, S. Dhillion, Soil function in a changing world: the role of invertebrate ecosystem engineers, Eur. J. Soil Biol. 33 (1997) 159–193.
[3] L. van Schaik, J. Palm, J. Klaus, E. Zehe, B. Schroder, Linking spatial earthworm distribution to macropore numbers and hydrological effectiveness, Ecohydrology 7 (2014) 401–408, https://doi.org/10.1002/eco.1358.
[4] K. Resner, K. Yoo, S.D. Sebestyen, A. Aufdenkampe, C. Hale, A. Lyttle, A. Blum, Invasive earthworms deplete key soil inorganic nutrients (Ca, Mg, K, and P) in a Northern hardwood forest, Ecosyst 18 (2015) 89–102, https://doi.org/10.1007/s10021-014-9814-0.
[5] S. Psarska, E.A. Nater, R.K. Kolka, Impacts of invasive earthworms on soil mercury cycling: two mass balance approaches to an earthworm invasion in a Northern Minnesota forest, Water Air Soil Pollut. 227 (2016) 205, https://doi.org/10.1007/s11270-016-2885-0.
[6] A. Martin, Short- and long-term effects of the endogeic earthworm Millsonia-Animala (Omodeo) (Megascolecidae, Oligochaeta) of tropical savannas, on soil organic matter, Biol. Fertil. Soils 11 (1991) 234–238.
[7] S. Angst, C.W. Mueller, T. Cajthaml, G. Angst, Z. Lhotakova, M. Bartuska, A. Spaldonova, J. Frouz, Stabilization of soil organic matter by earthworms is connected with physical protection rather than with chemical changes of organic matter, Geoderma 289 (2017) 29–35, https://doi.org/10.1016/j.geoderma.2016.11.017.
[8] Y. Capowiez, S. Cadoux, P. Bouchand, J. Roger-Estrade, G. Richard, H. Boizard, Experimental evidence for the role of earthworms in compacted soil regeneration based on field observations and results from a semi-field experiment, Soil Biol. Biochem. 41 (2009) 711–717, https://doi.org/10.1016/j.soilbio.2009.01.006.
[9] A.R. Taylor, L. Lenoir, B. Vegerfors, T. Persson, Ant and earthworm bioturbation in cold-temperate ecosystems, Ecosyst 22 (2019) 981–994, https://doi.org/10.1007/s10021-018-0317-2.
[10] A.C. Evans, LVII.—a method of studying the burrowing activities of earthworms, Ann. Mag. Nat. Hist. 14 (1947) 643–650.
[11] S.M.F. Cook, D.R. Linden, Effect of food type and placement on earthworm (Aporrectodea tuberculata) burrowing and soil turnover, Biol. Fertil. Soils 21 (1996) 201–206, https://doi.org/10.1007/BF00335936.
[12] E. Arrázola-Vásquez, M. Larsbo, Y. Capowiez, A. Taylor, M. Sandin, D. Iseskog, T. Keller, Earthworm burrowing modes and rates depend on earthworm species and soil mechanical resistance, Appl. Soil Ecol. 178 (2022), 104568, https://doi.org/10.1016/j.apsoil.2022.104568.
[13] M. Joschko, O. Graff, P.C. Muller, K. Kotzke, P. Lindner, D.P. Pretschner, O. Larink, A nondestructive method for the morphological assessment of earthworm burrow systems in 3 dimensions by X-ray computed-tomography, Biol. Fertil. Soils 11 (1991) 88–92.

[14] F. Bastardie, Y. Capowiez, J.R. de Dreuzy, D. Cluzeau, X-ray tomographic and hydraulic characterization of burrowing by three earthworm species in repacked soil cores, Appl. Soil Ecol. 24 (2003) 3–16, https://doi.org/10.1016/S0929-1393(03)00071-4.
[15] Y. Capowiez, S. Sammartino, E. Michel, Using X-ray tomography to quantify earthworm bioturbation non-destructively in repacked soil cores, Geoderma 162 (2011) 124–131, https://doi.org/10.1016/j.geoderma.2011.01.011.
[16] Y. Capowiez, S. Sammartino, T. Keller, N. Bottinelli, Decreased burrowing activity of endogeic earthworms and effects on water infiltration in response to an increase in soil bulk density, Pedobiologia 85–86 (2021), 150728, https://doi.org/10.1016/j.pedobi.2021.150728.
[17] F.J.R. Meysman, B.P. Boudreau, J.J. Middelburg, Relations between local, nonlocal, discrete and continuous models of bioturbation, J. Mar. Res. 61 (2003) 391–410.
[18] O. Maire, P. Lecroart, F. Meysman, R. Rosenberg, J.C. Duchene, A. Gremare, Quantification of sediment reworking rates in bioturbation research: a review, Aquat. Biol. 2 (2008) 219–238, https://doi.org/10.3354/ab00053.
[19] Y. Capowiez, F. Gilbert, A. Vallat, J.C. Poggiale, J.M. Bonzom, Depth distribution of soil organic matter and burrowing activity of earthworms-mesocosm study using X-ray tomography and luminophores, Biol. Fertil. Soils 57 (2021) 337–346, https://doi.org/10.1007/s00374-020-01536-y.
[20] H. Müller-Lemans, F. van Dorp, Bioturbation as a mechanism for radionuclide transport in soil: relevance of earthworms, J. Environ. Radioact. 31 (1996) 7–20.
[21] M.I. Zorn, C.A.M. Van Gestel, H. Eijsackers, The effect of Lumbricus rubellus and Lumbricus terrestris on zinc distribution and availability in artificial soil columns, Biol. Fertil. Soils 41 (2005) 212–215, https://doi.org/10.1007/s00374-004-0824-5.
[22] N.J. Jarvis, A. Taylor, M. Larsbo, A. Etana, K. Rosén, Modelling the effects of bioturbation on the re-distribution of 137Cs in an undisturbed grassland soil, Eur. J. Soil Sci. 61 (2010) 24–34, https://doi.org/10.1111/j.1365-2389.2009.01209.x.
[23] A.K. Covey, D.J. Furbish, K.S. Savage, Earthworms as agents for arsenic transport and transformation in roxarsone-impacted soil mesocosms: a μXANES and modeling study, Geoderma 156 (2010) 99–111, https://doi.org/10.1016/j.geoderma.2010.02.004.
[24] K. Yoo, J.L. Ji, A. Aufdenkampe, J. Klaminder, Rates of soil mixing and associated carbon fluxes in a forest versus tilled agricultural field: implications for modeling the soil carbon cycle, J. Geophys. Res.-Biogeosci. 116 (2011), https://doi.org/10.1029/2010JG001304.
[25] R.A. Wheatcroft, P.A. Jumars, C.R. Smith, A.R.M. Nowell, A mechanistic view of the particulate biodiffusion coefficient - step lengths, rest periods and transport directions, J. Mar. Res. 48 (1990) 177–207.
[26] K. Meurer, J. Barron, C. Chenu, E. Coucheney, M. Fielding, P. Hallett, A. M. Herrmann, T. Keller, J. Koestel, M. Larsbo, E. Lewan, D. Or, D. Parsons, N. Parvin, A. Taylor, H. Vereecken, N. Jarvis, A framework for modelling soil structure dynamics induced by biological activity, Global Change Biol. 26 (2020) 5382–5403, https://doi.org/10.1111/gcb.15289.
[27] T. Keller, T. Colombi, S. Ruiz, M.P. Manalili, J. Rek, V. Stadelmann, H. Wunderli, D. Breitenstein, R. Reiser, H. Oberholzer, S. Schymanski, A. Romero-Ruiz, N. Linde, P. Weisskopf, A. Walter, D. Or, Long-term soil structure observatory for monitoring post-compaction evolution of soil structure, Vadose Zone J. 16 (2017), https://doi.org/10.2136/vzj2016.11.0118.
[28] J. Klaminder, E.J. Krab, M. Larsbo, H. Jonsson, J. Fransson, J. Koestel, Holes in the tundra: invasive earthworms alter soil structure and moisture in tundra soils, Sci. Total Environ. 859 (2023), 160125, https://doi.org/10.1016/j.scitotenv.2022.160125.
[29] J.C. Alegre, B. Pashanasi, P. Lavelle, Dynamics of soil physical properties in Amazonian agroecosystems inoculated with earthworms, Soil Sci. Soc. Am. J. 60 (1996) 1522–1529, https://doi.org/10.2136/sssaj1996.03615995006000050033x.
[30] G.H. Baker, G. Brown, K. Butt, J.P. Curry, J. Scullion, Introduced earthworms in agricultural and reclaimed land: their ecology and influences on soil properties, plant production and other soil biota, Biol. Invasions 8 (2006) 1301–1316, https://doi.org/10.1007/s10530-006-9024-6.
[31] G. Blume-Werry, E.J. Krab, J. Olofsson, M.K. Sundqvist, M. Vaisanen, J. Klaminder, Invasive earthworms unlock arctic plant nitrogen limitation, Nat. Commun. 11 (2020), https://doi.org/10.1038/s41467-020-15568-3.
[32] D.A. Walker, M.K. Raynolds, F.J.A. Daniels, E. Einarsson, A. Elvebakk, W.A. Gould, A.E. Katenin, S.S. Kholod, C.J. Markon, E.S. Melnikov, N.G. Moskalenko, S. S. Talbot, B.A. Yurtsev, C. Team, The Circumpolar Arctic vegetation map, J. Veg. Sci. 16 (3) (2005) 267–282.
[33] A.A. Wackett, K. Yoo, J. Olofsson, J. Klaminder, Human-mediated introduction of geoengineering earthworms in the Fennoscandian arctic, Biol. Invasions 20 (2018) 1377–1386, https://doi.org/10.1007/s10530-017-1642-7.
[34] M.B. Bouché, Stratégies lombriciennes, in: U. Lohm, T. Persson (Eds.), Soil Organisms as Components of Ecosystems, vol. 25, Ecology Bulletin, Stockholm, 1977, pp. 122–132.
[35] N. Bottinelli, M. Hedde, P. Jouquet, Y. Capowiez, An explicit definition of earthworm ecological categories – marcel Bouché's triangle revisited, Geoderma 372 (2020), 114361, https://doi.org/10.1016/j.geoderma.2020.114361.
[36] M.J.I. Briones, R. Álvarez-Otero, Body wall thickness as a potential functional trait for assigning earthworm species to ecological categories, Pedobiologia 67 (2018) 26–34.
[37] A. Elzein, J. Balesdent, Mechanistic simulation of vertical distribution of carbon concentrations and residence times in soil, Soil Sci. Soc. Am. J. 59 (1995) 1328–1335, https://doi.org/10.2136/sssaj1995.03615995005900050019x.
[38] A. Le Couteulx, C. Wolf, V. Hallaire, G. Pérès, Burrowing and casting activities of three endogeic earthworm species affected by organic matter location, Pedobiologia 58 (2015) 97–103.
[39] Y. Capowiez, Differences in burrowing behaviour and spatial interaction between the two earthworm species Aporrectodea nocturna and Allolobophora chlorotica, Biol. Fertil. Soils 30 (2000) 341–346, https://doi.org/10.1007/s003740050013.
[40] F. Binet, P. Curmi, Structural effects of Lumbricus terrestris (oligochaeta: lumbricidae) on the soil-organic matter system: micromorphological observations and autoradiographs, Soil Biol. Biochem. 24 (1992) 1519–1523.
[41] D.J. Oyedele, P. Schjonning, A.A. Amusan, Physicochemical properties of earthworm casts and uningested parent soil from selected sites in southwestern Nigeria, Ecol. Eng. 28 (2006) 106–113, https://doi.org/10.1016/j.ecoleng.2006.05.002.
[42] J.W. Van Groenigen, K.J. Van Groenigen, G.F. Koopmans, L. Stokkermans, H.M. J. Vos, I.M. Lubbers, How fertile are earthworm casts? A meta-analysis, Geoderma 338 (2019) 525–535, https://doi.org/10.1016/j.geoderma.2018.11.001.
[43] E. Blanchart, A. Alain, J. Alegre, A. Duboisset, C. Villenave, B. Pashanasi, P. Lavelle, L. Brussaard, in: P. Lavelle, L. Brussard, P. Hendrix (Eds.), Effects of Earthworms on Soil Structure and Physical Properties, 1999, pp. 149–172.
[44] N. Bottinelli, J.L. Maeght, R.D. Pham, C. Valentin, C. Rumpel, Q.V. Pham, T. T. Nguyen, D.H. Lam, A.D. Nguyen, T.M. Tran, R. Zaiss, P. Jouquet, Anecic earthworms generate more topsoil than they contribute to erosion – evidence at catchment scale in northern Vietnam, Catena 201 (2021), 105186, https://doi.org/10.1016/j.catena.2021.105186.
[45] P. Barré, B.M. McKenzie, P.D. Hallett, Earthworms bring compacted and loose soil to a similar mechanical state, Soil Biol. Biochem. 41 (2009) 656–658, https://doi.org/10.1016/j.soilbio.2008.12.015.
[46] R Core Team, R: A Language and Environment for Statistical Computing, R Found. Stat. Comput., Vienna, 2022. http://www.R-project.org/.
[47] V. Wolters, Soil invertebrates - effects on nutrient turnover and soil structure - a review, Z. Pflanzenernahrung Bodenkd. 154 (1991) 389–402.
[48] J.M. Anderson, Invertebrate-mediated transport processes in soils, Agric. Ecosyst. Environ. 24 (1988) 5–19.
[49] J.P. Curry, O. Schmidt, The feeding ecology of earthworms – a review, Pedobiologia 50 (2007) 463–477, https://doi.org/10.1016/j.pedobi.2006.09.001.
[50] J.M. Perreault, J.K. Whalen, Earthworm burrowing in laboratory microcosms as influenced by soil temperature and moisture, Pedobiologia 50 (2006) 397–403, https://doi.org/10.1016/j.pedobi.2006.07.003.
[51] F. Bastardie, Y. Capowiez, P. Renault, D. Cluzeau, A radio-labelled study of earthworm behaviour in artificial soil cores in term of ecological types, Biol. Fertil. Soils 41 (2005) 320–327, https://doi.org/10.1007/s00374-005-0847-6.